IOSR Journal of Mechanical and Civil Engineering (IOSR-JMCE)
e-ISSN: 2278-1684,p-ISSN: 2320-334X, Volume 16, Issue 2 Ser. I (Mar. - Apr. 2019), PP 29-37
www.iosrjournals.org

An Analysis of the FEM Model of the Misaligned Rotational System with Rotational Looseness

Emir Nezirić[1], Safet Isić[1], Isak Karabegović[2], Avdo Voloder[3]
[1](*Faculty of Mechanical Engineering, "Džemal Bijedić" University of Mostar, Bosnia and Herzegovina)*
[2](*Technical Faculty, University of Bihać, Bosnia and Herzegovina)*
[3](*Faculty of Mechanical Engineering, University of Sarajevo, Bosnia and Herzegovina)*
Corresponding Author: Emir Nezirić

Abstract: *Knowing all characteristics of rotational system vibrations is most significant for a maintenance technician or engineer. Vibrations are carriers of a machine condition and by analysis of the vibration characteristics, it is possible to find what is the real cause of the vibrations. As a part of the research of rotational machinery vibrations, mathematical modeling of a rotational system is common tool before research is transferred to a real physical model. As an excellent method for this purpose, the best candidate could be a Finite Element Method. In this paper, an analysis of a Finite element model of rotational system motor – flexible coupling – rotor is presented. As a fault analyzed in this paper, misalignment and rotating looseness are modeled as external loads. For this FEM model of a rotational system is shown that it is suitable for the analysis of rotational machinery vibrations.*

Keywords: *FEM, frequency spectrum, orbit, rotating looseness, shaft alignment, waveform*

Date of Submission: 26-02-2019 Date of acceptance: 12-03-2019

I. Introduction

Shaft misalignment is the most often fault of the rotating machinery [1]. That is the main reason to increase the knowledge about its behavior and know how it impacts on the rotational machinery. It is possible to detect misalignment as machine fault by vibration measurement. Vibration characteristics of misaligned rotational systems are well-known in practical maintenance and are often one of the topics in the scientific researches. Main vibration characteristic of the misaligned rotational system is 1X and 2X order of rotational frequency in the frequency spectrum, and 3X up to 10X orders for severe misalignment [1, 2, 3, 4, 5].

Another rotational machinery fault which has similar frequency spectrum characteristics is rotational looseness. The main vibration characteristic of this fault is the multiple rotational frequency harmonics presence[6, 7]. Considering that both faults have similar frequency spectrum features, other vibration characteristics confirms the true vibration cause. To decide how each of the faults is affecting on the frequency spectrum and other characteristics of vibrations, it is necessary to investigate vibrations on the rotational machine with both of those faults present in the rotational system. Most researches are conducted with only one fault present in the rotational system and are very well documented. It is challenging to find the interaction of the mutual characteristics of the mentioned faults in the available literature. This paper is describing one step in the better understanding of the misalignment and rotational looseness vibrational characteristics interaction.

Investigating how those mentioned faults combination in the rotational machinery interacts on each other vibration characteristics should have the first step in setting up the appropriate theoretical model and carry out research on the model [8,9]. One of the best ways to define model is the finite element method (FEM) [10, 11]. In this paper, a FEM model of rotational system motor – flexible coupling – rotor with misalignment and rotational looseness as faults is analyzed. This presented model is solved with physical characteristics of the real rotational system. Analysis of vibrational data is presented in detail in this paper. The main goal of this paper is to point out the influence of the interaction of those faults on vibrational characteristics.

II. Description of the FEM model of misaligned rotational system with rotating looseness

The proposed system consists of a motor and rotor with a flexible shaft connected by a flexible coupling. To simplify the model, the motor shaft and motor bearings are considered rigid. Shaft with the rotor is flexible and is represented with 2D Euler-Bernoulli beam elements connected in series [10, 12]. The first node is at the beginning of the rotor shaft, and flexible coupling is connecting it to the motor shaft. One node which is on 1/3 of the shaft length is flexible bearing where rotating looseness would be introduced. In the last node on the shaft, the second flexible bearing would be defined. Flexible coupling and flexible bearings are introduced to model as external loads, which are dependent on node displacement.

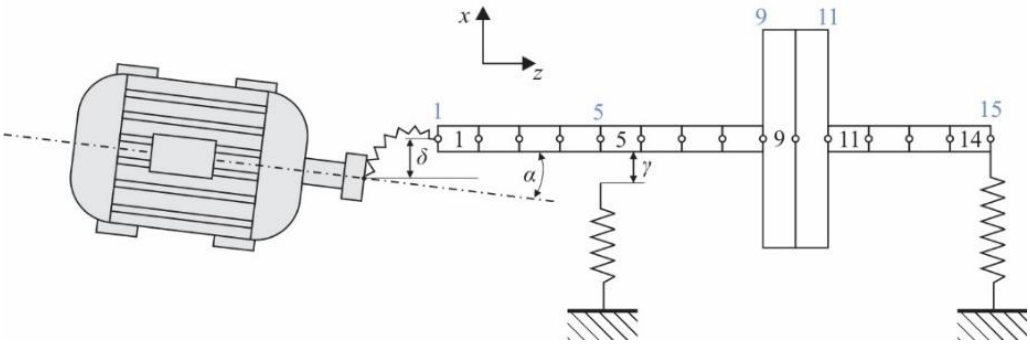

Fig.1. FEM model of misaligned rotational system with rotating looseness

Parallel and angular misalignment are used as faults which would cause lateral vibrations of the shaft. Rotating looseness is defined in the bearing closer to the coupling. Shaft node is free to move inside bearing until its displacement exceeds the value of a clearance between bearing outer ring and bearing housing. For this model, α and β represents angular misalignment in x-z and y-z plane respectively, δ represents parallel misalignment and γ represents bearing gap in loosened bearing.

Mass and stiffness matrices are described as Euler-Bernoulli elements. The centrifugal force is described by using the same shape functions as for Euler-Bernoulli elements with additional distance caused by misalignment.

Misalignment and rotating looseness are affecting the coupling and bearing deformations. Those deformations cause forces and bending moments in coupling and bearings. Generalized forces and moments could be obtained from the potential energy for nodes where coupling and bearings are introduced. Potential energy for coupling is

$$V_c = \frac{1}{2} k_c d_c^{\,2} \left(\sin(\alpha+\theta)\sin(\omega t) + \sin(\alpha+\theta)\right)^2 \tag{1}$$

where k_c is coupling stiffness, d_c is coupling diameter and θ is angular displacement of node where coupling is introduced. Potential energy for bearing in node 15 is

$$V_2 = \frac{1}{2} k_x \left((\delta + L_{b.2}\sin\alpha)(1-\cos(\omega t)) + u_{2x}\right)^2 + \frac{1}{2} k_y \left((\delta + L_{b.2}\sin\beta)\sin(\omega t) + u_{2y}\right)^2 \tag{2}$$

where k is bearing stiffness, $L_{b.2}$ is bearing 2 to coupling distance and u_2 is node displacement of bearing 2 (node 15).

Potential energy where the bearing 1 is introduced with rotating looseness depends on position of node inside the gap between the bearing and the housing. Potential energy of bearing 1 with gap is

$$V_1 = \begin{cases} \frac{1}{2} k \left((\delta + L_{b.1}\sin\alpha)(1-\cos(\omega t)) + u_1 - x'\right)^2 & x < x' \\ \frac{1}{2} k \left((\delta + L_{b.1}\sin\alpha)(1-\cos(\omega t)) + u_1 - x''\right)^2 & x > x'' \\ 0 & x' < x < x'' \end{cases} \tag{3}$$

where $x' = \delta + L_{b.1}\sin\alpha - \gamma$, $x'' = \delta + L_{b.1}\sin\alpha + \gamma$ and γ is gap between the bearing outer ring and the bearing housing.

Differentiating the potential energies of coupling and bearings is giving the generalized forces and moments vector and matrix. The vector of the generalized forces and moments has members at the positions which corresponds to displacements of nodes which belongs to bearings and coupling. Member of this vector which corresponds to the node where the bearing 1 is introduced is changing with node displacement, as shown in (3).

The matrix of the generalized forces and moments depends on generalized coordinates, and that is the reason it represents diagonal bearings and coupling stiffness matrix.

Generalized forces and moments vector and matrix are

$$\{\mathbf{R}_{\text{el.}}\} = \begin{Bmatrix} 0 \\ k_c d_c^{\,2}\alpha(\sin(\omega t)+1)^2 \\ \vdots \\ k((\delta + L_{b.1.}\sin\alpha)(1-\cos(\omega t))) \\ 0 \\ \vdots \\ k((\delta + L_{b.2.}\sin\alpha)(1-\cos(\omega t))) \\ 0 \end{Bmatrix}, \quad [\mathbf{K}_{el.}] = \begin{bmatrix} 0 & & & & & & \\ & k_c h & & & & & \\ & & \ddots & & & & \\ & & & k & & & \\ & & & & 0 & & \\ & & & & & \ddots & \\ & & & & & & k \\ & & & & & & & 0 \end{bmatrix} \tag{4}$$

where $h = d_c^{\,2}(\sin(\omega t)+1)^2$.

For the described rotational system equation of motion could be written as

$$[\mathbf{M}]\{\ddot{\mathbf{D}}\} + \left([\mathbf{K}] - [\mathbf{K}_{\Omega}] + [\mathbf{K}_{\text{el.}}]\right)\{\mathbf{D}\} = \{\mathbf{R}_{\Omega\delta}\} + \{\mathbf{R}_{\Omega\alpha}\} - \{\mathbf{R}_{\text{el.}}\} \tag{5}$$

where $\{\ddot{\mathbf{D}}\}$ and $\{\dot{\mathbf{D}}\}$ are acceleration and displacement vectors, [M] and [K] are mass and stiffness matrices for lateral displacement, $[K_{\Omega}]$ is centrifugal force stiffness matrix, $[K_{el.}]$ is diagonal matrix of bearings and coupling stiffness, $\{R_{\Omega\delta}\}$ and $\{R_{\Omega\alpha}\}$ are centrifugal force vectors and $\{R_{el.}\}$ is bearings and coupling elastic forces vector. Method of direct integration – the implicit method is used as a tool for solving this equation. Every step of the solution requires writing the equation of motion. The stiffness of the bearing with rotating looseness depends on the position of the bearing node and it is necessary to check does stiffness changes in transition between two consecutive steps. Part of the algorithm for (5) solution is

1. Check the position of the bearing 1 node inside the gap for step *n*.
   IF $D_n < \gamma \Rightarrow k = k_{bearing,}$
   ELSE $k = 0$
2. Calculate D_{n+1}
3. Check the position of the bearing 1 node inside the gap for step *n*+1.
   IF $D_n < \gamma$ *AND* $D_{n+1} < \gamma \Rightarrow k = k_{bearing}$ and go to next step
   ELSE IF $D_n < \gamma$ *AND* $D_{n+1} >= \gamma \Rightarrow k = k_{bearing}$ and go to step 1
   ELSE IF $D_n >= \gamma$ *AND* $D_{n+1} < \gamma \Rightarrow k = 0$ and go to step 1
   ELSE $k = 0$ and go to next step
4. Write D_{n+1} to file.

Bearing with the gap is behaving nonlinear and solution procedure requires checking the position of the node inside the gap, so the stiffness of the bearing is determined for the next step. This algorthm does not mentioning the steps which are related to the implicit method of direct integration, only the ones that are related to the solving nonlinearity of the bearing with rotational looseness.

III. Analysis of the FEM model of misaligned rotational system with rotating looseness

Proposed FEM model would be analyzed with physical characteristics which are taken from the real motor – coupling – rotor system. Physical characteristics are shown in table 1.

As faults in this rotational system would be used parallel misalignment (δ = 0.1 – 5.0 mm), angular misalignment (α = 0.001 – 0.005 rad) and bearing gap (γ = 0 – 0.4 mm), for which values would be analyzed vibration characteristics.

The Equation of motion is solved by inserting those numerical values of physical characteristics and then by application of the direct integration method for its solution. Values of vibration data (displacement) is stored in TXT file, and then imported in the data analysis software. Only analysis of the behavior of the 5th node is presented because all nodes have similar characteristics of vibrations.

Table 1: Physical characteristics of the motor-coupling-rotor system

Description	Symbol	Unit	Value
Modulus of elasticity	E	Pa	$200*10^9$
Shaft diameter	d	m	0.02
Rotor diameter	d_{rot}	m	0.20
Shaft length	L	m	0.35
Rotor length	L_{rot}	m	0.05
L1 to coupling distance	L_1	m	0.10
Rotor to coupling dist.	L_R	m	0.20
L2 to coupling distance	L_2	m	0.35

Material density	ρ	kg/m^3	7800.00
Bearing stifness	k_1, k_2	N/m	20*10^6
Coupling diameter	d_c	m	0.05

3.1. Analysis of parallel misalignment

The Equation of motion is solved with physical characteristics shown in table 1. and with different values of parallel misalignment. Fig. 2. shows displacement of node 5 and its frequency spectrum.

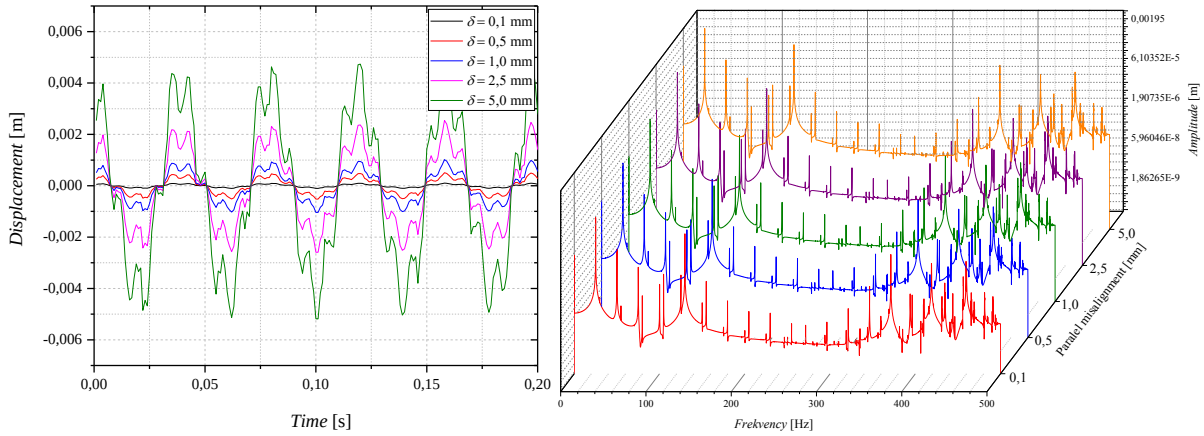

Fig. 2. Displacement (left) and Frequency spectrums waterfall plot (right) for node 5 (δ = 0.1 – 5.0 mm)

As shown on the left graph on Fig. 2., there is the characteristic shape of the vibration diagram for all parallel misalignment values. There are M and W shapes visible, where the only difference is the amplitude of vibrations. Also on other nodes, those shapes are noticeable. Fig. 2 shows frequency spectrums waterfall plot for the node 5 displacements for different values of parallel misalignment. As could be seen in Fig. 2., frequency spectrum has 1X (rotational frequency) and its higher orders (2X, 3X, …, 9X). Presence of the orders of the rotational frequency confirms source of the vibrations as misalignment. The shape of frequency spectrums are not changing, parallel misalignment increment increase only the amplitude of each frequency. Similar behavior is registered in other nodes in both directions (x and y) and it would not be discussed in this paper.

The interesting thing to notice on the left graph in Fig. 2. is that the average value of vibration is changing with an increment of distance between shafts. Fig. 3. (left) shows how the value of the distance between shafts impacts on vibrations average value for different nodes.

It could be seen that the average values of vibrations are increasing proportionally to the increment of shaft distance. This data could be used to determine shaft parallel misalignment value, but it has some difficulties. Firstly, it should be known at least two values of average vibration value with known parallel misalignment. Besides that, that information could also depend on other machinery faults present in the system.
Fig. 3. (right) shows dependence of frequency spectrum amplitudes for some characteristic frequencies. It is shown for rotational frequency, its 2X order and 129 Hz, which could be noticed in waterfall graph. As could be seen, all amplitudes are increasing linearly. Frequency 129 Hz represents the natural frequency of the system.

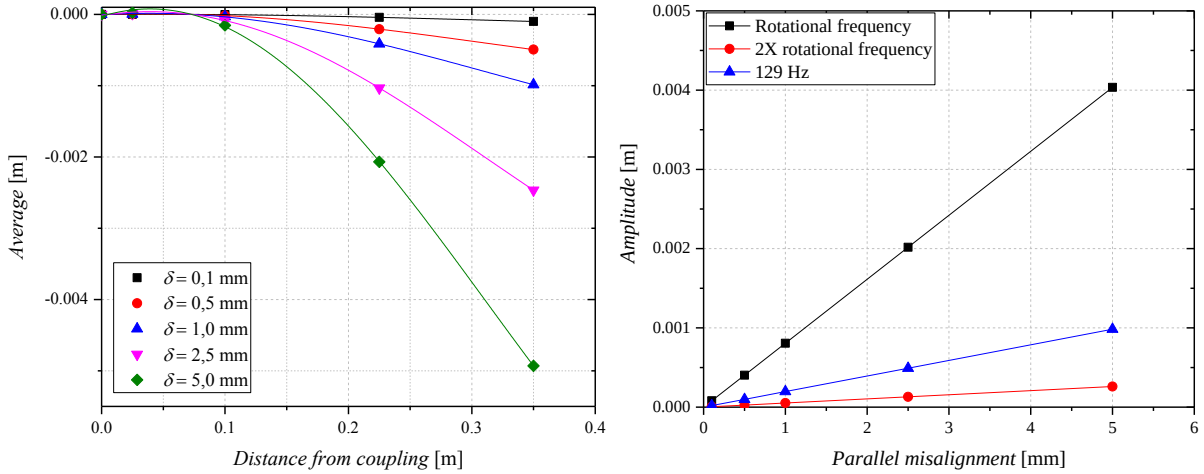

Fig. 3. Average value of vibration displacement for nodes 2, 5, 10 and 15 (left)

and amplitude of FFT peaks (right) for different parallel misalignment (δ = 0.1 – 5.0 mm)

Fig. 4. (left) shows orbits of nodes 2, 5, 10 and 15 with 0.1 mm od parallel misalignment, and orbit of node 5 with different values of parallel misalignment (right).

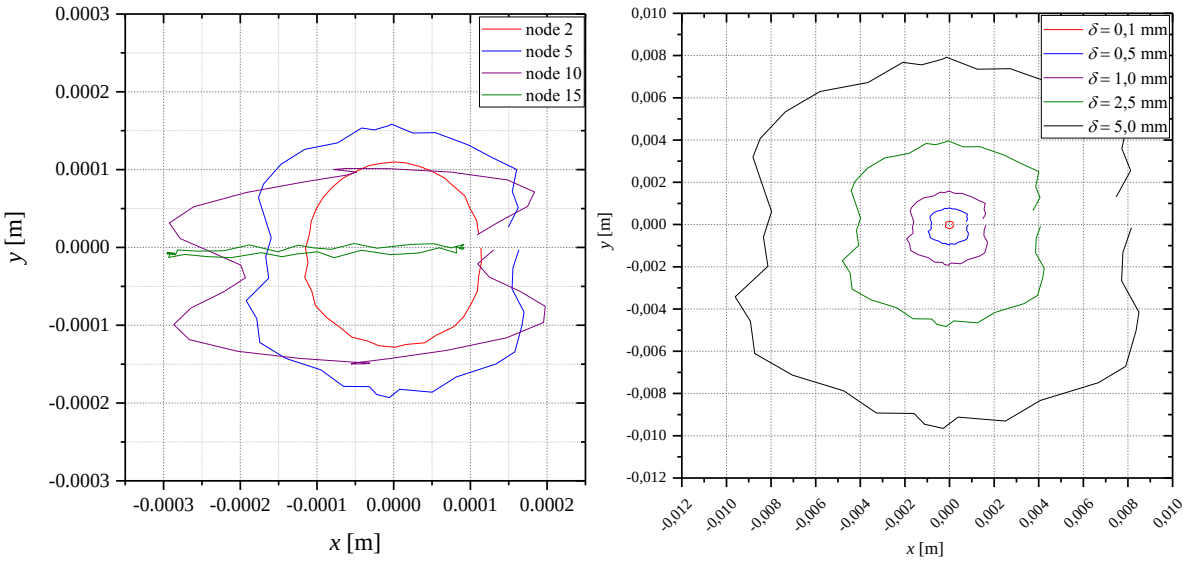

Fig. 4. Orbits of nodes 2, 5, 10 and 15 with 0.1 mm of parallel misalignment (left), and orbit of node 5 with different values of parallel misalignment (right).

As could be seen in Fig. 4., orbits are changing from node to node. Node 2 has almost circular shaped orbit since it is nearest to the coupling, and node 15 has mostly stretched shape of the orbit in *x*-direction. Orbits of nodes 5 and 10 are circular-like shaped with the narrowed central part of orbit in x-direction (8-shaped). It could be concluded that in presence of parallel misalignment, orbits could vary on a different position on the shaft.

Fig. 4. (right) shows that with the increment of parallel misalignment only dimensions of orbits are increased proportionally as amplitude. The shape of the orbit is not affected by parallel misalignment increment.

3.2. Analysis of angular misalignment

The equation of motion is solved with physical characteristics shown in table 1. and with different values of angular misalignment. Fig. 5. shows the displacement of node 5 and its frequency spectrum.

As it could be seen in Fig. 5., the presence of M and W shapes is noticeable. Also increase of amplitude is present with angular misalignment increment. Other nodes also have those characteristics in their displacement-time graphs.

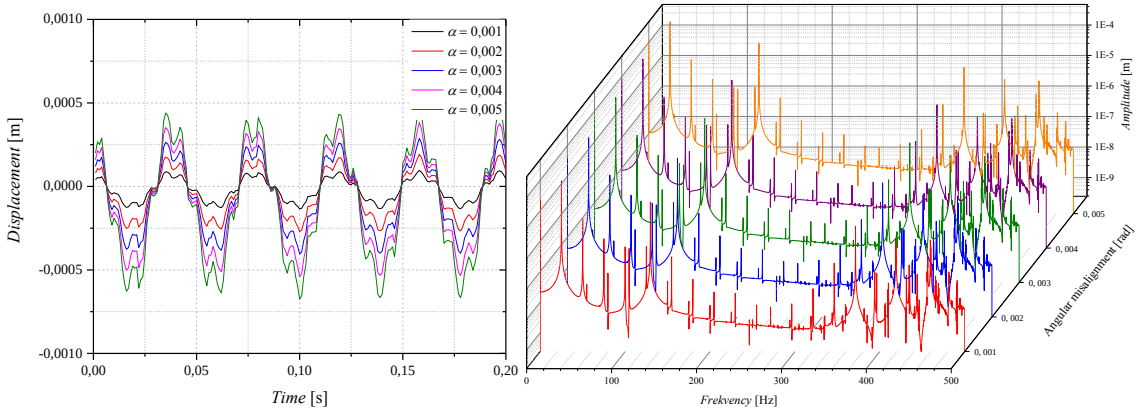

Fig. 5. Displacement (left) and Frequency spectrums waterfall plot (right) for node 5 (α = 0.001 – 0.005 rad)

Frequency spectrums for angular misalignment look pretty much same as frequency spectrum for parallel misalignment. Presence of rotating frequency with higher orders is frequency spectrum main characteristics. The only difference is that the higher orders have a higher amplitude for angular misalignment. Shapes of frequency spectrums are not changed with angular misalignment increment. Only amplitude is increased on frequency spectrums.

Fig. 6. shows average values of vibrations for different values of angular misalignment (left) and amplitude peaks of frequency spectrums for rotational frequency, its 2X order and systems natural frequency (right).

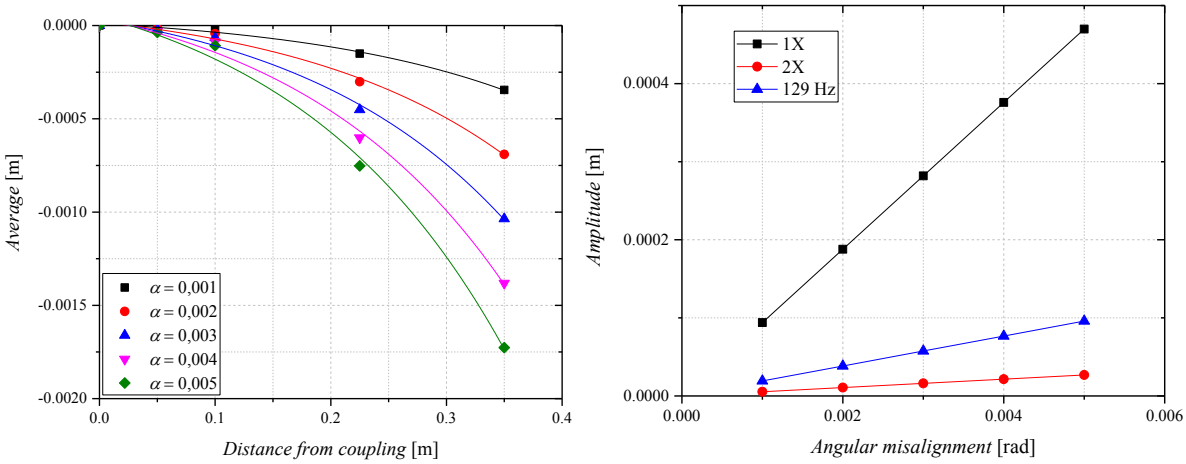

Fig. 6. Average value of vibration displacement for nodes 2, 5, 10 and 15 (left) and amplitude of FFT peaks (right) for different angular misalignment (α = 0.1 – 0v5 rad)

Similar as for parallel misalignment, the increment of average value of vibrations is proportionally increasing with the increment of angular misalignment. Also, the amplitudes of the rotational frequency, 2X order of rotational frequency and natural frequency are linearly increasing with the increment of angular misalignment. For these two characteristics, it could be concluded that parallel and angular misalingment have a similar impact on vibration characteristics.

Fig. 7. shows orbits for nodes 2, 5, 10 and 15 with 0.1 rad of angular misalignment (left), and orbits of node 5 with different values of angular misalignment (right).

As it could be seen on Fig. 7., shape of orbits are similar as with parallel misalignment. Only node 15 has different shape with angular misalignment and it is elliptical shaped. Also what could be seen is that orbit get wider in both directions for nodes that have larger distance from coupling. Shape of orbits for nodes 5 and 10 are similar to shape of orbits in case of parallel misalignment (8-shaped). Also the shape of the orbit (as shown on Fig. 7. on the right) is not affected by increment of angular misalignment. Only dimensions of orbits are proportionally increased with angular alignment.

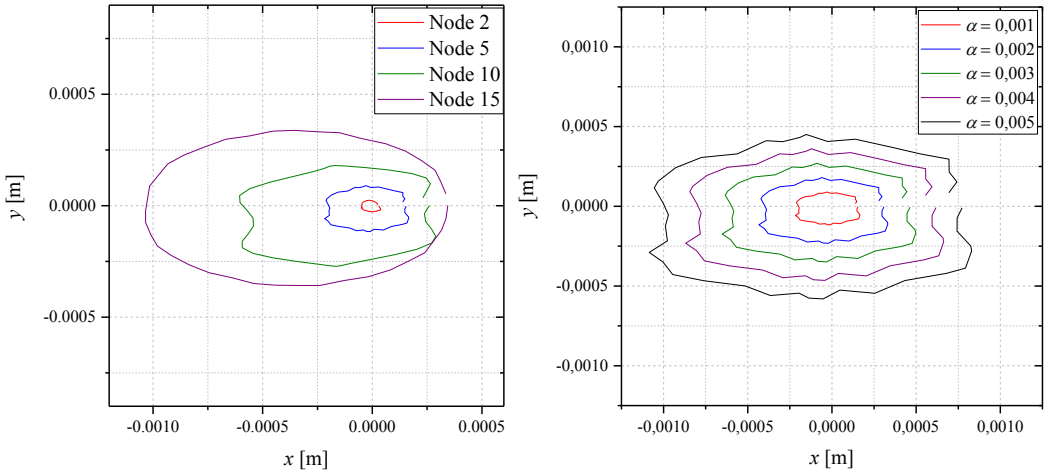

Fig. 7. Orbits of nodes 2, 5, 10 and 15 with 0.1 rad of angular misalignment (left), and orbits of node 5 with different values of angular misalignment (right).

3.3. Analysis of rotating looseness

Equation of motion with the shown characteristics in Table 1. and with 0-0,4 mm of bearing gap is solved for displacement values during 10 second period. In Fig. 8. is shown displacement of node 5 during 0.2 second period for different bearing gap values. Since the rotating loosensess is not a problem by itself, parallel misalignment of 0.1 mm is used as the initial fault that would cause vibrations.

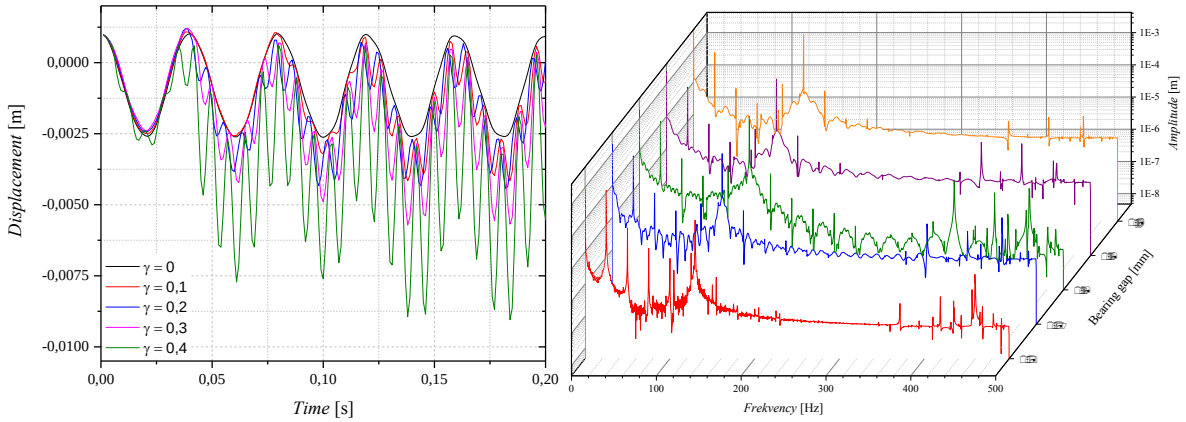

Fig. 8. Displacement (left) and Frequency spectrums waterfall plot (right) for node 5 (γ = 0 – 0.4 mm)

Vibrations of the node 5 are significantly affected by the increment of the bearing-housing gap. The amplitude of the displacement is increasing disproportionately to bearing-housing gap increment. Also, the shapes of W and M are not present, even parallel misalignment is used as disturbance in the rotational system.

Increasing the bearing-housing gap, the floor noise is also increased. Since the floor noise raises it hides the presence of the rotational frequency and its orders. The natural frequency amplitude to floor noise ratio is decreasing with bearing-housing gap increment, which means that unpredictable behaviour of the node inside the bearing-housing gap is trying to hide all usual characteristics of the misaligned rotational system.

Fig. 9. shows average values of vibrations for different values of the bearing-housing gap (left) and amplitude peaks of frequency spectrums for rotational frequency, its 2X order and systems natural frequency for different bearing-housing gaps (right).

The average value is significantly influences on the average value of vibrations. Difference between misalignments and rotating looseness modelled as the bearing-housing gap is that increment of the gap is not proportional to average value of vibrations. Also, the average value of node 15 is lower than the value of nodes 5 and 10 for gap value higher or equal to 0.1 mm. It is hard to describe average values dependence for each nodes.

Amplitudes of the analyzed peaks for node 5 vibrations are changing in cubic-like function. Change of natural frequency amplitude is more noticeable than the amplitude of the rotational frequency and its 2X order.

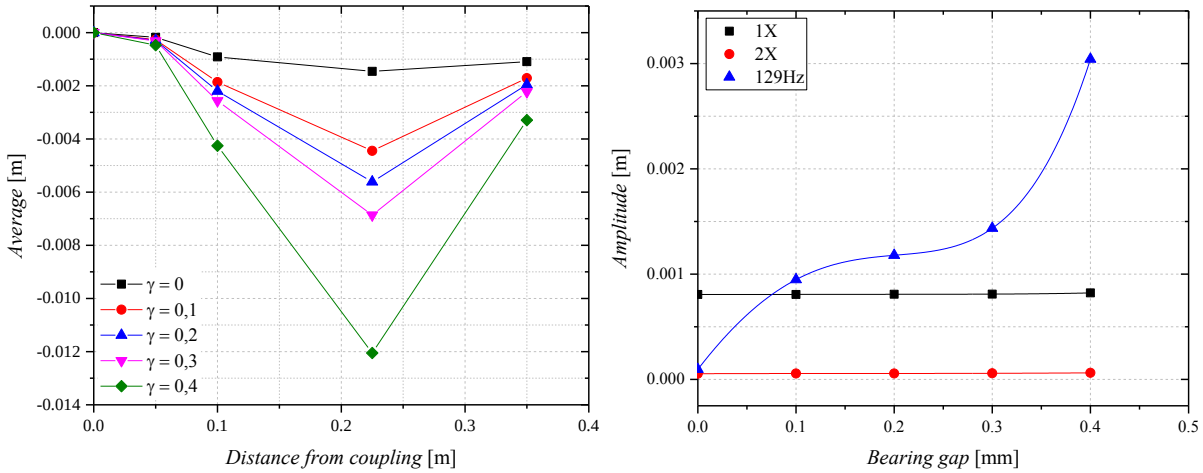

Fig. 9. Average value of vibration displacement for nodes 2, 5, 10 and 15 (left) and amplitude of FFT peaks (right) for different bearing-housing gaps (γ = 0 – 0.4 mm)

Fig. 10. shows orbits for nodes 5 and 15 with different values of the bearing-housing gap (right).

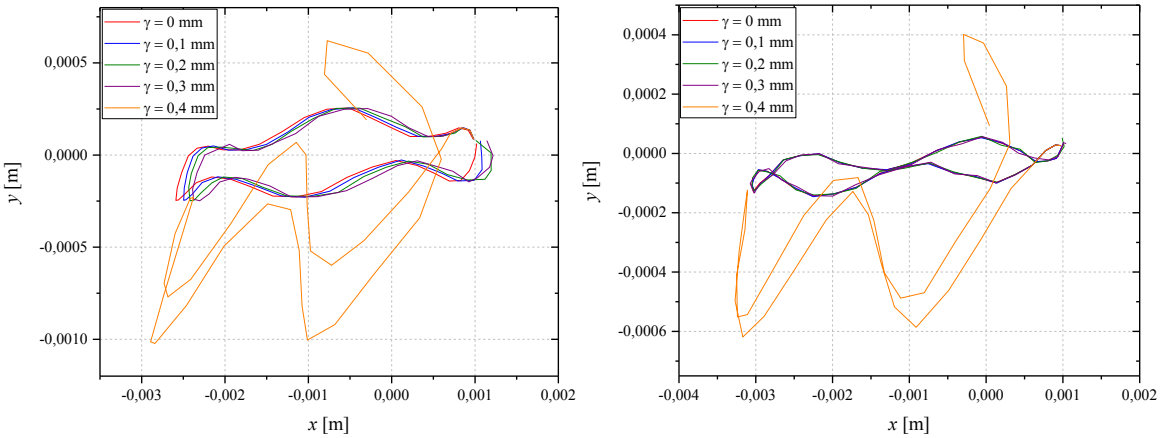

Fig. 10. Orbits for nodes 5 (left) and 15 (right) with different values of bearing-housing gap

The orbit of node 5 is elongated in *x*-direction, as expected since the bearing-housing gap is defined in this direction. Orbits are not changed with gaps values lower than 0.4 mm. Only for value of gap 0.4 mm, the orbit is changed, and as it could be seen, heavily affected by a bearing-housing gap. Movement of the node is unpredictable because when the gap is increased from 0 mm to 0.3 mm there was no significant change, and next increment from 0.3 mm to 0.4 mm of bearing-housing gap causes a notable change in orbit shape. Similar behaviour is present in orbit for node 15.

IV. Conclusion

Described analysis and discussion of a proposed model of the misaligned rotational system with rotational looseness induce following conclusions:

- Proposed FEM model of the misaligned rotational system with rotating looseness is convenient for analysis of misalignment and rotational looseness. This model could be used for modelling other rotational machinery faults by only changing the parts of the equation of motion which depends on loads.

- Characteristics of vibrations which are specific for misalignment are more noticeable in the position that is closer to the coupling on the shaft. Bending moments in coupling are the main reason for high orders of rotational frequency in the spectrum. Flexible coupling could reduce the impact of misalignment on the rotational system.

- Movement of the shaft inside bearing which has a gap between the outer ring and bearing housing (or shaft and the inner ring of bearing) is unpredictable. Phase measurement, which is common in vibration analysis practices, could not be performed accurately.

- Presence of rotating looseness in system increase floor noise in the frequency spectrum. Floor noise in the frequency spectrum could be so increased that it could also hide higher orders of rotational frequency.

- Orbits of each node have different shape and dimensions. Some nodes are slightly 8 shaped, and some are elliptic. By increasing misalignment, an increase of orbit dimensions is proportional to increment of misalignment, and shape is not changing. By introducing rotational looseness to the bearing, the orbit is affected that it does not have any significant impact on size or shape. That is the case until the value of bearing-housing gap passes some value “critical” to that system. After that, the orbit is unstable and unpredictable.

- Information gathered by this research could be a valuable source of knowledge for vibration analyst or future experimental research on this topic since the combination of the analyzed faults in this paper is frequent in common rotational machinery.

References

[1]. J. Piotrovski, *Shaft Alignment Handbook* (Boca Raton, FL: CRC Press, 2007)

[2]. M. Xu, R.D. Marangoni, Vibration analysis of a motor-flexible coupling-rotor system subject to misalignment and unbalance, Part I: Theoretical model and analysis, *Journal of Sound and Vibration, 176(5)*, 1994, 663-679.

[3]. M. Xu, R.D. Marangoni, Vibration analysis of a motor-flexible coupling-rotor system subject to misalignment and unbalance, Part II: Experimental validation, *Journal of Sound and Vibration, 176(5)*, 1994, 681-691.

[4]. E. Nezirić, S. Isić, V. Doleček, I. Karabegović, Vibration analysis of theoretical SDOF model of shaft parallel misalifnment, *Journal Technolog, 5(4/2014)*, 2014, 131-134.

[5]. E. Nezirić, S. Isić, V. Doleček, I. Karabegović, Impact of bearing and coupling stifness on characteristics of rotary system vibrations, *Proc. 11th International Symposium on Stability, Vibration, and Control of Machines and Structures*, Belgrade (Serbia), 2014, 119-129.

[6]. X. Li, The Analysis of vibration fault features and vibration mechanism caused by rotating machinery loosening, *Advanced Materials Research, vols. 518-523*, 2012, 3826-3829.

[7]. C. Scheffer, P. Girdhar, *Machinery vibration analysis & predictive maintenance* (Oxford, UK: Elsevier Science and Technology, 2004)
[8]. M.L. Adams, *Rotating machinery vibration: from analysis to troubleshooting* (Boca Raton, FL: Taylor and Francis Group, 2010)
[9]. G. Genta, *Dynamics of rotating systems* (New York: Springer Science+Business Medina inc., 2005)
[10]. E. Nezirić, S. Isić, I. Karabegović, A. Voloder, FEM model of misaligned rotational system with rotating looseness, *New Technologies, Development and Application. NT 2018. Lecture Notes in Networks and Systems, vol. 42*, 2019, 135-143.
[11]. A.Y.T. Leung, Spinning finite elements, *Journal of sound and vibration, 125(3)*, 1988, 523-537.
[12]. V. Doleček, A. Voloder, S. Isić, *Vibracije* (Sarajevo, BA: Faculty of Mechanical engineering, 2009).

Emir Nezirić. "An Analysis of the FEM Model of the Misaligned Rotational System with Rotational Looseness." IOSR Journal of Mechanical and Civil Engineering (IOSR-JMCE) , vol. 16, no. 2, 2019, pp. 29-37